



Proceeding Paper

A Methodological Approach to Identify Thermal Anomaly Hotspots Misclassified as Fire Pixels in Fire Radiative Power (FRP) Products [†]

Federico Filippini ^{1,2,*}  and Alessandro Mercatini ²

¹ National Research Council—Institute of Environmental Geology and Geoengineering (CNR-IGAG), Strada Provinciale 35d, 9-00010 Montelibretti, RM, Italy

² Italian Institute for Environmental Protection and Research (ISPRA), Via Vitaliano Brancati 48, 00144 Roma, Italy; alessandro.mercatini@isprambiente.it

* Correspondence: federico.filippini@cnr.it

[†] Presented at the 5th International Electronic Conference on Remote Sensing, 7–21 November 2023; Available online: <https://ecrs2023.sciforum.net/>.

Abstract: Thermal anomalies detected by Earth observation satellites have been widely used to identify active fires, even though there has been a high percentage of misclassified fire pixels. A total of about 75,000 Fire Radiative Power (FRP) pixels have been spatially and temporally combined with the EFFIS Burned Areas Database, distributed under the Copernicus Emergency Management Service, in order to identify thermal anomaly hotspots misclassified as fire pixels. The proposed approach uses a cluster analysis to partition the FRP pixels dataset into discrete subsets, based on defined distance measures like the spatial distance of the pixel centroids and the temporal frequencies. Later, zonal statistics were performed in order to evaluate fractional land cover within each identified hotspot. Results demonstrate that misclassified large surfaces, like industrial areas, can be identified from both spatial and temporal patterns, while other FRP false alarms are smaller in size.

Keywords: fire radiative power; thermal anomalies; wildfires



Citation: Filippini, F.; Mercatini, A. A Methodological Approach to Identify Thermal Anomaly Hotspots Misclassified as Fire Pixels in Fire Radiative Power (FRP) Products. *Environ. Sci. Proc.* **2024**, *29*, 47. <https://doi.org/10.3390/ECRS2023-16316>

Academic Editor: Riccardo Buccolieri

Published: 21 November 2023



Copyright: © 2023 by the authors. Licensee MDPI, Basel, Switzerland. This article is an open access article distributed under the terms and conditions of the Creative Commons Attribution (CC BY) license (<https://creativecommons.org/licenses/by/4.0/>).

1. Introduction

Wildfires are frequent across Italy, and satellite observation represents a valid tool to detect and assess the spread of wildfires. Unfortunately, only a fraction of fires are observed by satellites, many of which are too small to be detected or are masked by clouds. In addition, in some cases the duration of fires is too short as compared to satellites' revisit time. In most cases, the energy emitted through radiative processes released during combustion (Fire Radiative Power—FRP) can be associated with fire intensity [1] and used as a proxy for the fire. On the other hand, active fire data assessments of FRP anomalies, other than fire burning due to both anthropogenic structures (like industrial areas, photovoltaic fields, and bright reflective roofs) and natural processes (such as volcanoes) can lead to false positives in the detection of active fires [2]. Permanent false-positive FRP pixels may recur during active fire detection due to their similarity to fires in brightness, temperature, and spectral reflectance.

Thermal anomalies detected by Earth's observation satellites have been widely used to identify active fires. FRP can be estimated from the radiance at medium wave infrared (3–5 μm) wavelengths, measured by multiple polar-orbiting and geostationary satellite sensors, and represents the instantaneous radiative energy that is released from actively burning fires. FRP has been used to support the mapping of burned scars, by identifying core areas and estimating trace gas and aerosol rates of emissions, hence strengthening the monitoring of wildfire activities and their impact on the environment and ecosystems [3]. Algorithms to operationally generate FRP products from Earth's observation satellite acquisitions in near real time account for background window statistics, corrections, adjustments,

and tests to eliminate false alarms, in order to distinguishing fire pixels from non-fire pixels. Nevertheless, a high percentage of thermal anomalies are misclassified as possible fire pixels.

This research study aims at presenting a methodological approach to identify thermal anomaly hotspots, misclassified as fire pixels. FRP products over Italian National territory, generated for the period 2022–2023 from SLSTR, MODIS and VIIRS satellite sensors and distributed by Copernicus, EUMETSAT and NASA FIRMS, have been collected and analyzed. Characteristics of FRP anomalies, other than fire-related combustion, were investigated in order to establish an approach for discriminating false-positive active fires, and to improve their recognition through spatio-temporal analysis. The experiment was carried out for the year 2022 and for the first seven months of the year 2023 (the latter period was used for a comparison exercise).

2. Materials and Methods

To carry out this study, two datasets for the period January 2022–July 2023 were used. The first one contains the active fire pixel data from the Fire Radiative Power–Near Real Time Database (FRP-NRTD), consisting of a list of geographic coordinates of individual active fire pixels centroids, hereafter named FRP points, combining various datasets (Table 1). FRP represents emissive estimates of thermal anomalies, derived from data acquired during daytime and nighttime satellite overpasses using passive optical sensors at medium wavelengths (3–5 μm). FRP provides quantitative information on the measurement of radiant heat, and is widely used as a proxy for fire events [4].

Table 1. Satellites and relative sensors used to generate the FRP-NRTD database (URLs accessed on 26 September 2023).

Satellite	Sensor	Resolution	URL
Aqua (EOS PM-1)	MODIS	1000 m	https://firms.modaps.eosdis.nasa.gov
Terra (EOA AM-1)	MODIS	1000 m	https://firms.modaps.eosdis.nasa.gov
SNPP	VIIRS	375 m	https://firms.modaps.eosdis.nasa.gov
Sentinel-3	SLSTR	1000 m	https://www.eumetsat.int/S3-NRT-FRP

The second dataset that was used was the Burnt Areas Database–Italian Terrestrial Ecosystems (BAD-ITE), a geodatabase containing spatially explicit information, which allows the quantitative analysis of the impact of the main fires in the spatial and temporal dimensions, with a specific focus on natural protected areas and terrestrial ecosystems in the Italian national territory. The BAD-ITE database was generated from the real-time updated Burnt Areas database, distributed by EFFIS (<https://effis.jrc.ec.europa.eu>, accessed on 26 September 2023), which contains spatial polygons that delimit the areas affected by fire, identified from satellite sensor acquisitions (MODIS Aqua, MODIS Terra, and Sentinel-2 MSI at spatial resolutions of 250 and 20 m), and contains time information related to fire events.

In addition, the Corine Land Cover Backbone 2018 thematic mapping product was used to perform zonal statistics for different land covers.

The first step used for clustering analysis (Figure 1) consists of labelling each of the about 75,000 FRP pixel points with a class, belonging to a legend reported in Table 2. Space is the leading dimension used for FRP point labelling, and each point is first checked as spatially residing within burned areas. Later, time information of burned areas, available from fields named ‘FIREDATE’ and ‘LASTUPDATE’ in BAD-ITE, is used to identify FRP points that occurred temporally during each mapped fire event (Figure 2). On the one hand, FRP products in Near Real-Time (NRT) mode may have spatial displacement, due to approximated estimates of azimuth angle and satellite positioning [5], spatially collocating FRP points outside actual burned area polygons. On the other hand, burned area polygons may have been mapped using a change detection method from satellite images acquired

few days after the fire took place, resulting in temporal information lagging behind the actual fire date. To find the best spatial buffer radius and time lag values, accounting for the above-mentioned constraints, a sensitivity analysis of FRP point labelling with respect to burned areas' spatial buffer radius (range 0–2000 m) and temporal lag (range 0–96 h) was performed.

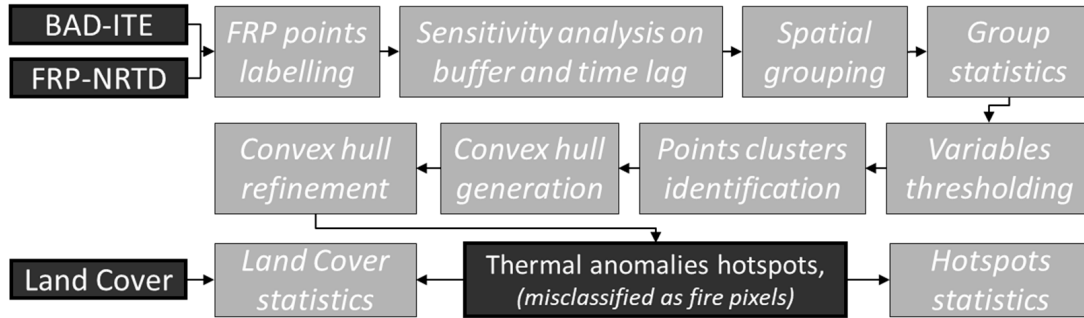


Figure 1. Flowchart for the FRP points analysis.

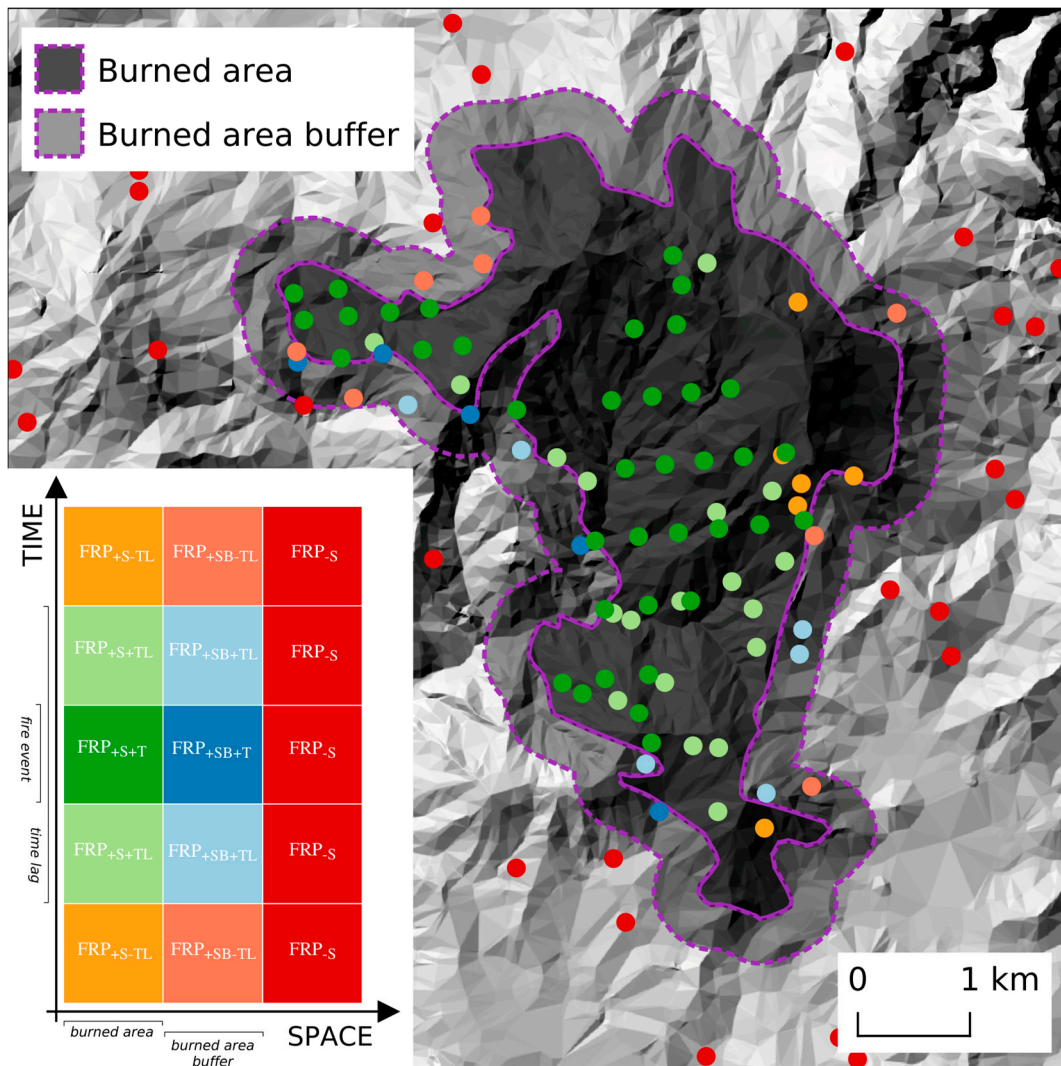


Figure 2. Map of the different FRP point classes, based on spatial and temporal overlay with burned areas. Plot representing classes' positions in space and time dimensions.

The second step used for clustering analysis allowed the FRP points dataset to be partitioned into discrete subsets, based on a statistical analysis of the points’ spatial distance and temporal frequencies. For each FRP point, a spatial buffer with a radius 1000 m was used to identify the group of surrounding FRP points and compute group statistics. Specifically, variables used for clustering were the number of FRP points within the spatial buffer and the number of singular days of year that each FRP point in the group had been sensed by satellites. For each variable, a threshold value was selected by comparing variable values’ distributions for the different FRP points classes, in order to spatially identify points clusters that can be considered thermal anomaly hotspots, misclassified as fire pixels. For each points cluster, the corresponding spatial convex hull has been generated. Later, with the aim of refining thermal anomaly hotspot borders, avoiding more isolated points, only areas with more than 3 overlapping convex hulls were used to generate the final hotspots polygons.

Finally, zonal statistics were performed in order to evaluate fractional land cover within each identified hotspot.

3. Results and Discussion

Based on sensitivity analysis results, the spatial buffer radius from burned area polygons used for subsequent analysis was set to 400 m, and the time lag set to 26 h (Figure 3).

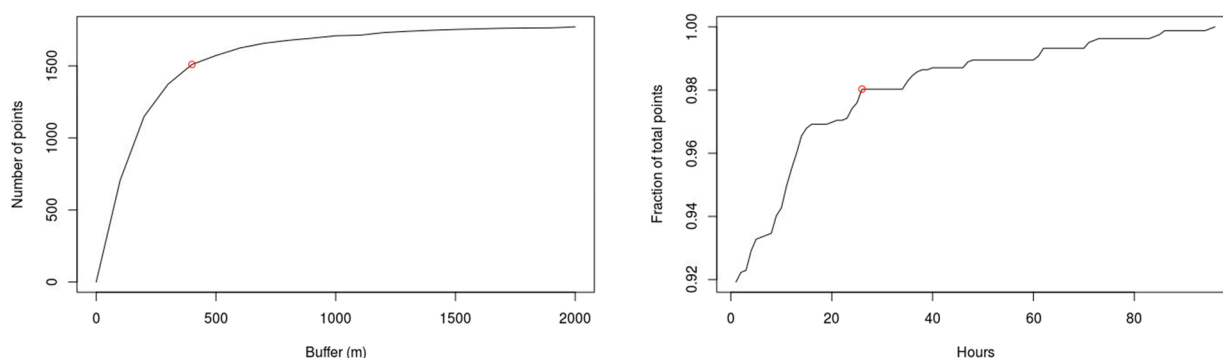


Figure 3. Spatial buffer radius and time lag sensitivity analysis plots.

The combination of the spatio-temporal information of burned area polygons and FRP points allowed us to assign each point to a specific class, identifying which FRP points are potentially related to the fire and which others are false positives. Results reported in Table 2 show that about 85% of FRP points did not match any fire event.

Table 2. Statistics for FRP point class legend.

Class	Description	Count	Percentage
FRP _{-S}	Outside burned area polygon	42,670	83.61
FRP _{+S-TL}	Inside burned area polygon, outside fire event time lag	329	0.64
FRP _{+S+T}	Inside burned area polygon, within fire event time range	2397	4.70
FRP _{+S+TL}	Inside burned area polygon, within fire event time lag	1590	3.12
FRP _{+SB-TL}	Inside burned area buffer polygon, outside fire event time lag	1590	1.17
FRP _{+SB+T}	Inside burned area buffer polygon, within fire event time range	1510	2.96
FRP _{+SB+TL}	Inside burned area buffer polygon, within fire event time lag	1939	3.80

From the spatial intersection between the burned area polygons and FRP points, with corresponding spatial buffer and time lag, 79.01% of burned areas had an FRP point sensed by satellites during fire events in 2022. A comparison exercise with January 2023–July 2023

acquisitions resulted in 77.88% of corresponding points (77.67% from the same year period in 2022).

Based on variable values distributions for the different FRP points classes, threshold value for the number of points in a group was set to 100 and the threshold value for the number of singular days of year was set to 10 (Figure 4). Overlay statistics of convex hulls allowed us to finally identify 120 thermal anomaly hotspots misclassified as fire pixels.

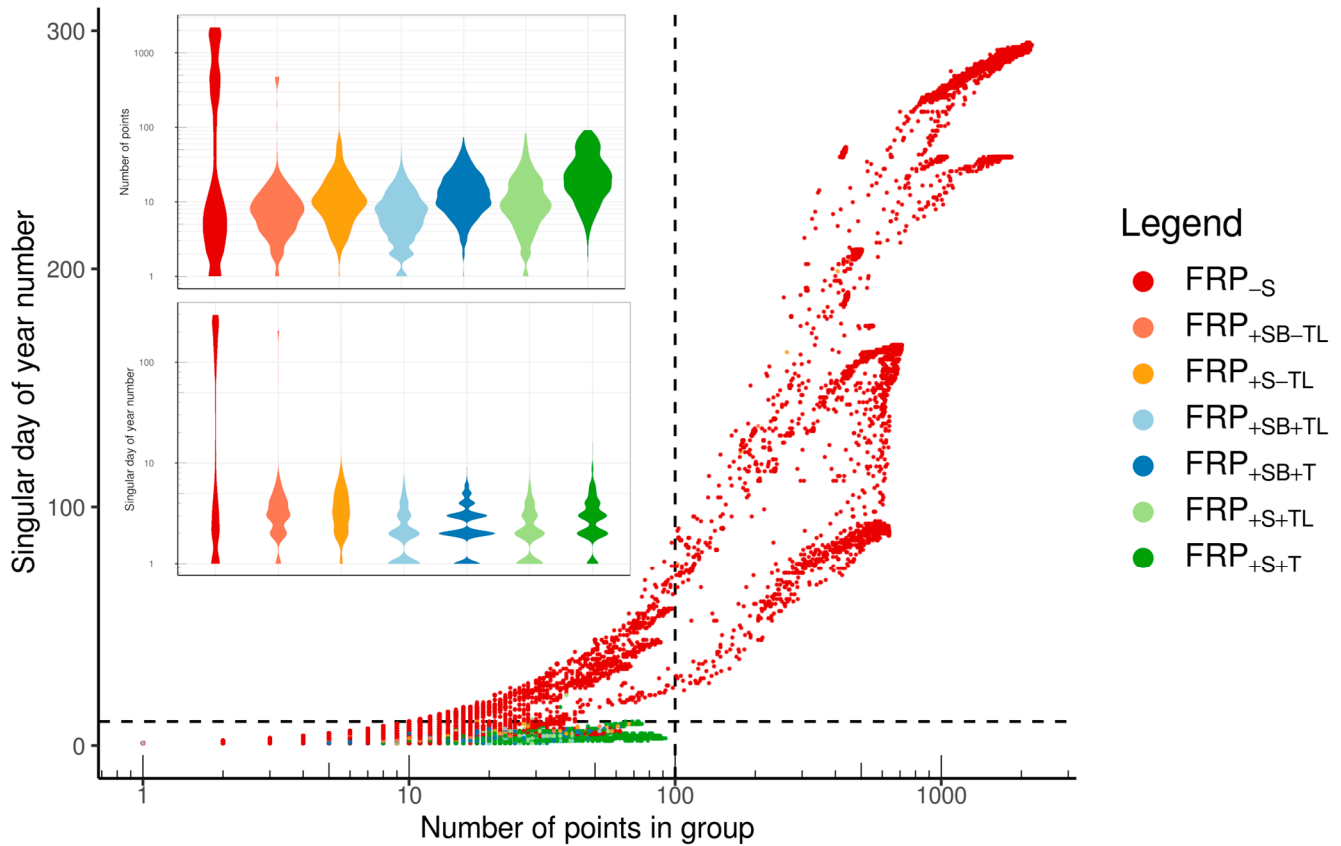


Figure 4. FRP points scatterplot relative to the number of points in the group and number of singular days of year. Distribution of number of points in group and number of singular days of year according to legend classes.

Identified hotspots (Figure S1), although they are a small number and correspond to about 165 km² (0.05% of Italian national territory), allow the removal of about 40% of misclassified FRP points (Table 3). A comparisons exercise using 2023 data showed that four FRP points fell within burned areas in 2023, which overlapped the thermal anomalies hotspot of misclassified fire pixels identified from the 2022 data analysis. These points were located in a single grassland area where a fire event occurred in the surroundings of a large industrial area.

Table 3. Number of FRP points and statistics on removed misclassified FRP points.

Temporal Period	FRP Points Number	Number of Misclassified FRP Points			Number of Removed Misclassified FRP Points			Percentage of Removed Misclassified FRP Points		
		(FRP _{-S})	(FRP _{+S-TL})	(FRP _{+SB-TL})	(FRP _{-S})	(FRP _{+S-TL})	(FRP _{+SB-TL})	(FRP _{-S})	(FRP _{+S-TL})	(FRP _{+SB-TL})
1 January 2022 31 December 2022	51,033		43,597		16,428		37.68			
1 January 2022 31 July 2022	32,732		27,485		11,637		42.34			
1 January 2023 31 July 2023	23,386		18,817		7686		40.85			

From a comparison with land cover classes (Figure 5), identified thermal anomaly hotspots were characterized by a high cover percentage of a sealed surface. From a visual inspection of the geolocation of the hotspots, it has been possible to observe that they are mainly located in correspondence with industrial areas, metallurgical industries, cement factories, warehouses, and volcanoes. Herbaceous cover had higher cover percentage values compared to other vegetation cover classes, suggesting that trying to use exclusively sealed surfaces to generate a mask to remove FRP pixels in anthropic areas could not be sufficient. This likely happened because of approximated estimates of azimuth angle and satellite positioning in the NRT product, which may generate FRP point horizontal displacements in the order of hundreds of meters.

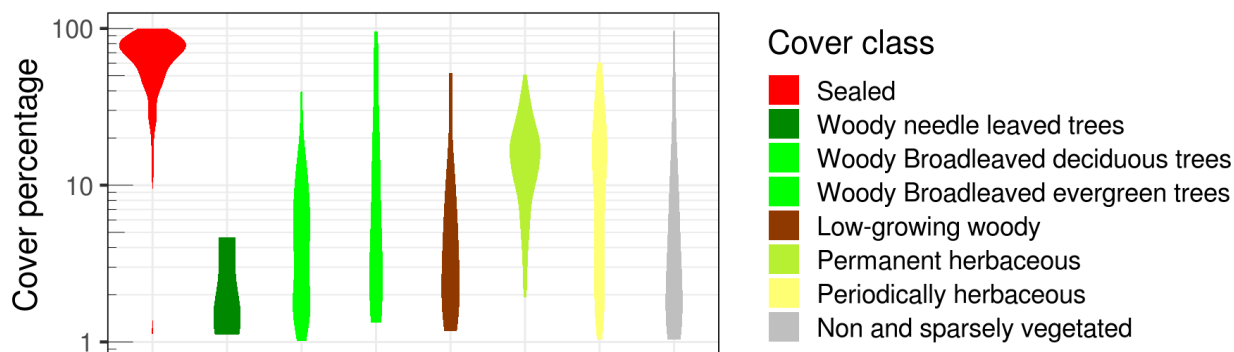


Figure 5. Violin plot for land cover classes percentage within identified hotspots.

The presented approach shows the capability for identifying thermal anomaly hotspots and reducing by about 40% the number of misclassified fire pixels in order to generate static masks for FRP products post-processing, improving the capacity of FRP products in providing prompt and accurate information for operational services addressing the monitoring of wildfires and their impact on the environment and ecosystems.

Supplementary Materials: The following supporting information can be downloaded at: <https://www.mdpi.com/article/10.3390/ECRS2023-16316/s1>, Figure S1: Distribution map of identified thermal anomaly hotspots.

Author Contributions: Conceptualization, F.F. and A.M.; methodology, F.F. and A.M.; formal analysis, F.F. and A.M.; data curation, F.F. and A.M.; writing—original draft preparation, F.F.; writing—review and editing, F.F. and A.M. All authors have read and agreed to the published version of the manuscript. The authors of this research contributed equally to this work.

Funding: This research received no external funding.

Institutional Review Board Statement: Not applicable.

Informed Consent Statement: Not applicable.

Data Availability Statement: BAD-ITE is publicly available at the following link: <https://groupware.sinanet.isprambiente.it/prodotti-operativi-di-sorveglianza-ambientale/library/disturbance-agents/wildfires/burnt-areas-italian-terrestrial-ecosystem> (accessed on 26 September 2023).

Conflicts of Interest: The authors declare no conflicts of interest.

References

1. Barrett, K.; Kasischke, E.S. Controls on variations in MODIS fire radiative power in Alaskan boreal forests: Implications for fire severity conditions. *Remote Sens. Environ.* **2013**, *130*, 171–181. [[CrossRef](#)]
2. Sofan, P.; Fajar, Y.; Anjar, D.S. Characteristics of False-Positive Active Fires for Biomass Burning Monitoring in Indonesia from VIIRS Data and Local Geo-Features. *ISPRS Int. J. Geo-Inf.* **2022**, *11*, 601. [[CrossRef](#)]
3. Li, F.; Zhang, X.; Kondragunta, S.; Schmidt, C.C.; Holmes, C.D. A preliminary evaluation of GOES-16 active fire product using Landsat-8 and VIIRS active fire data, and ground-based prescribed fire records. *Remote Sens. Environ.* **2020**, *237*, 111600. [[CrossRef](#)]

4. Hernandez, C.; Keribin, C.; Drobinski, P.; Turquety, S. Statistical modelling of wildfire size and intensity: A step toward meteorological forecasting of summer extreme fire risk. *Ann. Geophys. Eur. Geosci. Union* **2015**, *33*, 1495–1506. [[CrossRef](#)]
5. Freeborn, P.H.; Wooster, M.J.; Roy, D.P.; Cochrane, M.A. Quantification of MODIS fire radiative power (FRP) measurement uncertainty for use in satellite-based active fire characterization and biomass burning estimation. *Geophys. Res. Lett.* **2014**, *41*, 1988–1994. [[CrossRef](#)]

Disclaimer/Publisher’s Note: The statements, opinions and data contained in all publications are solely those of the individual author(s) and contributor(s) and not of MDPI and/or the editor(s). MDPI and/or the editor(s) disclaim responsibility for any injury to people or property resulting from any ideas, methods, instructions or products referred to in the content.